Functionalization of Nanoscale Diamond Powder: Fluoro-, Alkyl-, Amino-, and Amino Acid-Nanodiamond Derivatives

Yu Liu, Zhenning Gu, John L. Margrave,† and Valery N. Khabashesku*

Department of Chemistry and the Center for Nanoscale Science and Technology, Rice University, 6100 Main Street, Houston, Texas 77005-1892

Received July 10, 2004

The reaction of nanoscale diamond (ND) powder with an elemental fluorine/hydrogen mixture at temperatures varying from 150 to 470 °C resulted in the high degree of ND surface fluorination yielding a fluoro-nanodiamond with up to 8.6 at. % fluorine content. The fluoro-nanodiamond was used as a precursor for preparation of the series of functionalized nanodiamonds by subsequent reactions with alkyllithium reagents, diamines, and amino acids. The fluoro-nanodiamond and corresponding alkyl-, amino-, and amino acid-nanodiamond derivatives were characterized by scanning electron microscopy (SEM), transmission electron microscopy (TEM), X-ray diffraction (XRD), Fourier transformed infrared (FTIR) and X-ray photoelectron spectroscopy (XPS), and thermal gravimetry-mass spectrometry (TG-MS) measurements. In comparison with the pristine nanodiamond, all functionalized nanodiamonds show an improved solubility in polar organic solvents, e.g., alcohols and THF, and a reduced particle agglomeration. The developed methodology provides an efficient method for the chemical modification of nanodiamond powder, which enables a variety of engineering and biomedical applications of ND derivatives.

Introduction

Diamond has become one of the most important materials for science and technology due to its exhibited combination of extreme hardness, chemical inertness, low electrical and high thermal conductivities, wide optical transparency, and other unique properties.[1,2] Diverse applications of diamond materials have been facilitated by the mid-1950s discovery and subsequent development of processes for the large-scale production of the synthetic diamonds.[2] These industrial processes mostly employ high-pressure−high-temperature technologies to produce a single-crystalline diamonds, while at the laboratory scale methods of physical and chemical vapor deposition of polycrystalline diamond films are commonly used. These diamond materials have been traditionally applied as abrasives and cutting tools and also as substrates in microelectronics. In recent years, a number of synthetic methods for preparation of nanocrystalline diamond, "nanodiamond" (ND), in the form of films and powders have been developed.[3,4] Particularly, detonation synthesis from powerful explosive mixtures[5−7] has made the nanodiamond powder commercially available in ton quantities which enabled many engineering applications and also prompted a search for new application fields of diamond.[4]

Nanodiamond powders prepared by explosive techniques present a novel class of nanomaterials possessing unique surface properties. Due to the very small particle size (2−10 nm), a larger percentage of atoms in nanodiamonds are contributing to the defect sites on grain boundaries than in single crystal natural or microcrystalline synthetic diamonds. For example, in the individual 4.3 nm size spherical particles of ND, consisting of about 7200 carbon atoms, nearly 1100 atoms are located on the surface.[3] For this reason, the surface modifications of the nanosize diamond grains can affect the bulk properties of this material more strongly than those of micro- and macroscale diamonds. For example, nanodiamond powders can form good abrasive pastes and suspensions for high-precision polishing; nanodiamond−polymer composites are applied for manufacturing aircraft, cars, and ships as well as in hard and wear-resistant surface coatings. They are considered as potential medical agents due to high adsorption capacity, high specific surface area, and chemical inertness.[3,4] Applications of nanodiamond thin films were demonstrated in the fabrication of cold cathodes, field emission displays,[8−12] and nanomechanical and nanoelectro-

* Corresponding author. E-mail: khval@rice.edu.
† Deceased.

(1) Wilks, E.; Wilks, J. *Properties and Applications of Diamond*; Butterworth: Oxford, England, 1997.
(2) Pierson, H. O. *Handbook of Carbon, Graphite, Diamond and Fullerenes*; Noyes Publ.: Park Ridge, NJ, 1993.
(3) Shenderova, O. A.; Zhirnov, V. V.; Brenner, D. W. *Crit. Rev. Solid State Mater. Sci.* **2002**, *27*, 227.
(4) Dolmatov, V. Y. *Russ. Chem. Rev.* **2001**, *70*, 607.
(5) Greiner, N. R.; Phillips, D. S.; Johnson, J. D.; Volk, F. *Nature* **1988**, *333*, 440.
(6) Vereschagin, A. L.; Sakovich, G. V.; Komarov, V. F.; Petrov, E. A. *Diamond Relat. Mater.* **1993**, *3*, 160.
(7) Kuznetsov, V. L.; Chuvilin, A. L.; Moroz, E. M.; Kolomiichuk, V. N.; Shaikhutdinov, Sh. K.; Butenko, Yu. V. *Carbon* **1994**, *32*, 873.
(8) Alimova, A. N.; Chubun, P. I.; Detkov, P. Y.; Zhirnov, V. V. *J. Vac. Sci. Technol., B* **1999**, *17*, 715.
(9) Show, Y.; Witek, M. A.; Sonthalia, P.; Swain, G. M. *Chem. Mater.* **2003**, *15*, 879.
(10) Choi, W. B.; Cuomo, J. J.; Zhirnov, V. V.; Myers, A. F.; Hren, J. J. *Appl. Phys. Lett.* **1996**, *68*, 720.

10.1021/cm048875q CCC: $27.50
Published on Web 09/02/2004

mechanical resonant structures (NEMS)[13−15] and were suggested for the design of biosensors as stable biologically active substrates after DNA modification.[16]

To minimize the surface energy, the individual ND particles of 4−6 nm size structurally self-organize into clusters or primary aggregates of 20−30 nm size, which in turn form larger weakly bonded secondary aggregates ranging from hundreds of nanometers to micrometer sizes. This agglomeration is likely facilitated by surface functional groups, such as COOH, OH, SO_3H, and NH_2, which are created along with the other functionalities by the chemical treatment processing of detonation ND[3,17] and participate in the formation of hydrogen bonds between nanodiamond clusters. However, for advanced applications of ND powder, e.g. in higher precision polishing compositions, nanoengineered electronic devices, polymer and ceramic composites, and biomedical systems, the reduction of aggregate sizes to below 200 nm, and ultimately even to single clusters or particles, and the availability of specific functional groups on the surface is highly desirable. These functional groups can also serve as binding sites for covalent integration of ND into polymer structures and provide for improved solubility of ND powder in common solvents. Surface modification of the ND powder particles through a selective surface chemistry should be instrumental in approaching these goals. In this work we have developed the chemical methodology for selective functionalization of nanodiamond powders. This methodology is based on covalent modification of the nanodiamond particle surface by direct fluorination to form a "fluoro-nanodiamond" in which fluorine can be displaced by a variety of organic groups, e.g., alkyl, aryl, or those terminated with hydroxyl, carboxyl, or amino moieties, to produce a series of nanodiamond derivatives.

Diamond surface modification has been studied during the past decade,[16,18−28] and fluorination was regarded as an efficient way to modify and control the surface properties.[26,29−33] However, all previous work was done either on larger size (micrometer scale) polycrystalline diamond[25,28−30] or on thin films[16,18−24,26,27,31] grown in a vacuum chambers and no further chemistry, utilizing the C−F bond reactivity in particular, was pursued after fluorination. In this paper, we report the surface modification of nanoscale diamond powder through chemical treatment, first with a mixture of fluorine and hydrogen gases at elevated temperatures (150−470 °C) and then by reacting the resulting fluoro-nanodiamond **(1)** precursor with selected alkyllithium reagents, diamines, and amino acids (Scheme 1). The displacement of fluorine accompanied by intermolecular elimination of LiF or HF in the course of these reactions results in corresponding methyl-, *n*-butyl-, hexyl-, ethylenediamino-, and glycine-functionalized nanodiamond derivatives **(2a−e)**, which all show an improved solubility in comparison with the untreated nanodiamond. Herein, we provide a full report on the syntheses and characterization data of these derivatives. Some of these data we only briefly presented earlier at meetings.[34]

Scheme 1

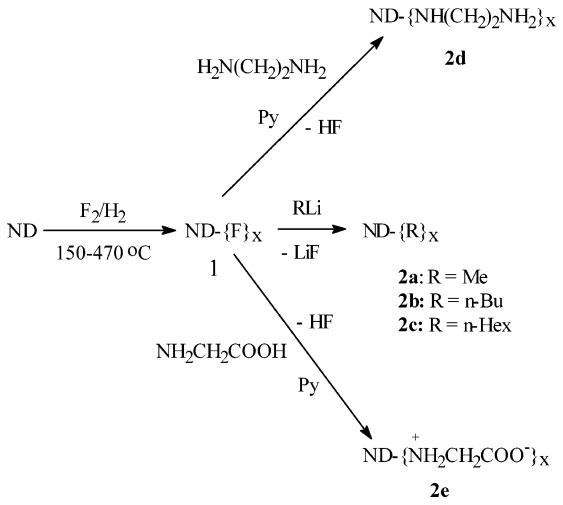

Experimental Section

Materials and Methods. Nanodiamond powder with phase purity higher than 97% (<2.5% graphite and amorphous carbon, 0.1−0.15% Fe, 0.1−0.3% Si) and particle sizes ranging from 3.5 to 6.5 nm was purchased from the Nanostructured and Amorphous Materials, Inc. The alkyllithium reagents (2 M solutions in diethyl ether, cyclohexane, or hexane), ethylenediamine, and glycine ethyl ester hydrochloride were supplied by Aldrich. Fluorine was purchased from Spectra Gases.

(11) Ralchenko, V.; Karabuto, A.; Vlasov, I.; Frolov, V.; Konov, V.; Gordeer, S.; Zhukov, S.; Dementjev, A. *Diamond Relat. Mater.* **1999**, *8*, 1496.
(12) Jiang, N.; Eguchi, K.; Noguchi, S.; Inaoka, T.; Shintani, Y. *J. Cryst. Growth* **2002**, *236*, 577.
(13) Wang, J.; Butler, J. E.; Hsu, D. S. Y.; Nguyen, C. T.-C. *Proc. 15th IEEE Int. Conf. Micro Electromechan. Syst.* **2002**, 657.
(14) Sekaric, L.; Parpia, J. M.; Craighead, H. G.; Feygelson, T.; Houston, B. H.; Butler, J. E. *Appl. Phys. Lett.* **2002**, *81*, 4455.
(15) Philip, J.; Hess, P.; Feygelson, T.; Butler, J. E.; Chattopadhyay, S.; Chen, K. H.; Chen, L. C. *J. Appl. Phys.* **2003**, *93*, 2164.
(16) Yang, W.; Auciello, O.; Butler, J. E.; Cai, W.; Carlisle, J. A.; Gerbi, J. E.; Gruen, D. M.; Knickerbocker, T.; Lasseter, T. L.; Russel, J. N., Jr.; Smith, L. M.; Hamers, R. J. *Nat. Mater.* **2002**, *1*, 253.
(17) Jiang, T.; Xu, K.; Ji, S. *J. Chem. Soc., Faraday Trans.* **1996**, *92*, 3401.
(18) Hamers, R. J.; Coulter, S. K.; Ellison, M. D.; Hovis, J. S.; Padowitz, D. F.; Schwartz, M. P. *Acc. Chem. Res.* **2000**, *33*, 617.
(19) Bent, S. F. *Surf. Sci.* **2002**, *500*, 879.
(20) Hukka, T. I.; Pakkanen, T. A.; D'Evelyn, M. P. *J. Phys. Chem.* **1994**, *98*, 12420.
(21) Hovis, J. S.; Hamers, R. J.; D'Evelyn, M. P.; Russell, J. N., Jr.; Butler, J. E. *J. Am. Chem. Soc.* **2000**, *122*, 732.
(22) Wang, G. T.; Bent, S. F.; Russell, J. N., Jr.; Butler, J. E.; D'Evelyn, M. P. *J. Am. Chem. Soc.* **2000**, *122*, 744.
(23) Fitzgerald, D. R.; Doren, D. J. *J. Am. Chem. Soc.* **2000**, *122*, 12334.
(24) Hossain, M. Z.; Aruga, T.; Takagi, N.; Tsuno, T.; Fujimori, N.; Ando, T.; Nishijima, M. *Jpn. J. Appl. Phys.* **1999**, *38*, L1496.
(25) Miller, J. B.; Brown, D. W. *Langmuir* **1996**, *12*, 5809.
(26) Smentkowski, V. S.; Yates, J. T., Jr. *Science* **1996**, *271*, 193.
(27) Kim, C. S.; Mowrey, R. C.; Butler, J. E.; Jr. Russell, J. N. *J. Phys. Chem. B* **1998**, *102*, 9290.
(28) Nakamura, T.; Ishihara, M.; Ohana, T.; Koga, Y. *Chem. Commun.* **2003**, 900.
(29) Ando, T.; Yamamoto, K.; Matsuzawa, M.; Takamatsu, Y.; Kawasaki, S.; Okino, F.; Touhara, H.; Kamo, M.; Sato, Y. *Diamond Relat. Mater.* **1996**, *5*, 1021.
(30) Kealey, C. P.; Klapötke, T. M.; McComb, D. W.; Robertson, M. I.; Winfield, J. M. *J. Mater. Chem.* **2001**, *11*, 879.
(31) Ando, T.; Tanaka, J.; Ishii, M.; Kamo, M.; Sato, Y.; Ohashi, N.; Shimosaki, S. *J. Chem. Soc., Faraday Trans.* **1993**, *89*, 3105.
(32) Touhara, H.; Okino, F. *Carbon* **2000**, *38*, 241.
(33) (a) Ferro, S.; De Battisti, A. *J. Phys. Chem. B* **2003**, *107*, 7567. (b) Ferro, S.; De Battisti, A. *Anal. Chem.* **2003**, *75*, 7040.
(34) (a) Liu, Y.; Agrawal, N.; Gu, Z.; Peng, H.; Khabashesku, V. N.; Margrave, J. L. *Abstracts of Papers*, Rice Quantum Institute 16th Annual Summer Research Colloquium; Aug 9, 2002, Houston, TX; Rice University: Houston, TX; p 2. (b) Khabashesku, V. N. Presented at the Fuctionalization of Carbon Nanomaterials for Bio-Medical Applications in Proceedings of International Meeting of German Society of Gerontology and Geriartrics: Extending the Life Span, Sep 24−26, 2003, Hamburg, Germany.

Fluorination. In a typical fluorination process, 200 mg of nanodiamond powder was placed into a monel reactor that was continuously purged with helium. The reactor was heated by the temperature-controlled hot plate to a selected temperature, 150, 310, 410, or 470 °C, and then the loaded sample was annealed at that temperature for about 3−4 h. After that, fluorine and hydrogen gases were separately introduced into the reactor at a controlled 3:1 flow rate ratio. The purpose of using hydrogen in the process was to generate HF in situ, which is thought to catalyze the fluorination reaction of surface functional groups on nanodiamond. The fluorination was continued for 48 h. Thereafter, the reactor was cooled to room temperature, flows of hydrogen and fluorine gases were stopped, and the resulting gray-colored fine powder of fluoro-nanodiamond **(1)** was unloaded from the reactor. The weights of the material produced at each fluorination temperature were practically the same, about 195 mg.

Subsequent Functionalizations. The fluorinated nanodiamond powder was used as a precursor in the subsequent functionalizations through reactions with several types of organic nucleophilic reagents—alkyllithium compounds, diamines, and amino acids. For preparation of alkyl-nanodiamond derivatives **2a**−**c**, e.g., hexyl-nanodiamond **(2c)**, 50 mg of **1** was added to 50 mL of dry hexane in a 250 mL flask under nitrogen atmosphere. The contents were sonicated with the 17 W/55 kHz Cole Palmer bath for 5 min and then cooled in ice. Thereafter, 10 mL of hexyllithium reagent (2.3 M solution in dry hexane) was added dropwise to the resulting suspension and the mixture was sonicated for 20 min followed by stirring overnight under nitrogen and then cooling in ice. The unreacted hexyllithium was quenched by slow addition of ethanol while stirring. After that, water was added to dissolve the salts formed. The powder product was filtered and resuspended in 3 N HCl by sonication for 10 min. Finally, the nanodiamond derivative **2c** was filtered out, washed with plenty of water and ethanol, and then dried in a vacuum oven at 70 °C for 12 h to yield a fine light-brown powder. Methyl- *and n*-butyl-nanodiamond derivatives, **2a**,**b**, respectively, were prepared via a similar procedure.

Amino-nanodiamond derivative **(2d)** was prepared by refluxing 50 mg of **1** in 50 mL of anhydrous ethylenediamine in the presence of pyridine at about 130 °C for 24 h under nitrogen atmosphere. After cooling of the mixture to room temperature, the final product was filtered off, washed with plenty of water and ethanol, and then dried in a vacuum oven at 70 °C overnight yielding a dark-brown powder of **2d**.

For preparation of glycine-nanodiamond derivative **(2e)** 50 mg of **1** was sonicated in 100 mL of *o*-dichlorobenzene for 20−30 min. Then 200 mg of glycine ethyl ester hydrochloride and several drops of pyridine were added and the mixture was stirred at ∼130−140 °C for 8−12 h. The resulting black-colored product **2e** was filtered off, washed with a large amount of ethanol, and vacuum-dried at 70 °C overnight.

Characterization. Pristine nanodiamond powder and the derivatives **2a**−**e** were characterized by using a series of available materials characterization methods— ATR-FTIR, XRD, XPS, TGA and TG-MS, SEM/EDX, TEM, and dynamic light scattering (DLS) analyses. The ATR-FTIR spectral measurements were done using a Thermo Nicolet Nexus 670 FTIR system with an ATR accessory. X-ray diffraction data were collected on a GADDS powder diffractometer equipped with a Cu Kα radiation source. XPS data were obtained with the help of a Physical Electronics PHI 7500 X-ray photoelectron spectrometer using an Al Kα radiation source (1486.6 eV) with a power setting of 350 W and an analyzer pass energy of 23.5 eV. The thermal degradation analyses were performed with a TA-SDT-2960 TGA-DTA analyzer. The gaseous and volatile products formed were identified with the help of TG-MS technique using TA Q-series 500 instrument coupled to a Pfeiffer Thermostar quadrupole mass spectrometer. Argon was always used in the TG-MS runs as a purge gas.

Scanning electron microscopy (SEM) was performed at 30 kV beam energy using a Phillips XL-30 field emission microscope equipped with an energy-dispersive X-ray (EDX) analyzer. Transmission electron microscopy (TEM) photoimages of the specimen placed on lacey carbon coated copper grids (size 200 mesh) were obtained with a JEOL JEM-2010 electron microscope operating at an accelerating voltage of 100 kV. Measurements of the particle size distribution in the solutions were performed using a Coulter N4 PLUS instrument.

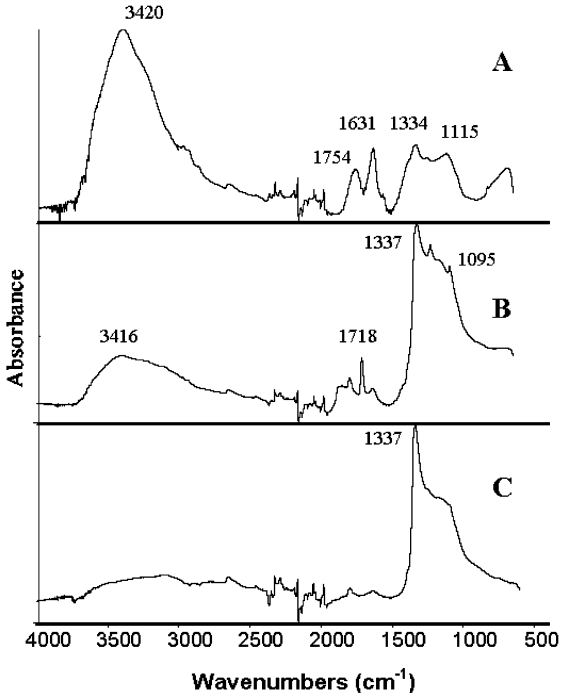

Figure 1. ATR-FTIR spectra of nanodiamond powder for pristine (A) and fluorinated at temperatures 150 °C (B) and 310 °C (C).

Results and Discussion

Fluorination of Nanodiamond Powder. In comparison with the recent fluorination studies of polycrystalline diamond powder (with mean particle sizes of about 1 μm),[30,32] in this work a nanocrystalline powder, having tiny average particle sizes (∼3.5 nm), was utilized. The BET surface area, measured for this "as-supplied" ND powder material (245 m^2/g), is much higher than that for 1 μm-sized polycrystalline diamond (13−15 m^2/g). Also, unlike previous studies,[30,32] in our work the powder samples were not pretreated by hydrogenation or oxidation at high temperatures prior to fluorination. Accordingly, the fluorination reactions mainly involved the already existing surface functionalities, which have been activated by the in situ generated HF catalyst.

The ATR-FTIR spectrum of the ND powder (Figure 1A) shows a strong absorption at 3420 cm^{-1}, medium-intensity shoulder peaks in the 2800−3000 cm^{-1} region, and bands at 1754, 1631, 1334, 1260, and 1115 cm^{-1} due to the O−H, C−H, C═O, C═C, and C−O stretching and bending deformation modes of the hydroxyl, carboxylic acid, and the anhydride, carbonyl, CH, and C═C surface functional groups. The energy dispersive X-ray analysis (EDX) data yield about 10 wt % oxygen content in the ND sample, which is consistent with the IR spectroscopy results showing the dominant presence of the oxygenated functionalities.

Fluorination of the ND powder at 150 °C already results in a product showing an IR spectrum (Figure 1B) significantly different from that of the starting

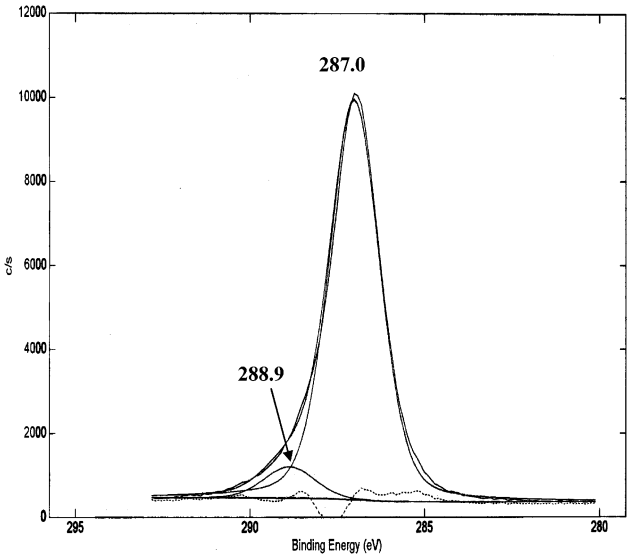

Figure 2. Deconvoluted C 1s peak in the XPS spectrum of fluoro-nanodiamond: XRD patterns of nanodiamond (a) and hexyl-nanodiamond (b) powders.

material. The absorption due to the O−H stretches shows at 3416 cm^{-1} and is dramatically weakened in this spectrum, while new bands appear at 1865, 1800, and 1718 cm^{-1}, characteristic of the C═O stretchings of various F-substituted carbonyl groups[35] on the ND surface. The new strong peaks are also observed in the C−F stretch region at 1337, 1234, 1173, 1095, and 966 cm^{-1}. The absence of the bands which belong to stretching vibrations of the C−H bonds should be particularly noted. This indicates that at 150 °C these bonds become entirely fluorinated. In accord with the IR data, EDX analysis shows 5 at. % fluorine and a reduced to 1.2 at. % oxygen contents in the sample fluorinated at this temperature.

At a higher temperature (310 °C), almost all O−H, C═O, and C═C groups are removed or transformed by fluorination, resulting in the notable increase in peak intensity (Figure 1C) of the C−F stretching vibrations in the 1100−1400 cm^{-1} range.[29,31,32] EDX data indicate an increase of the fluorine content in the sample to 6.5 at. % that proves the additional surface fluorination. Elevation of the fluorination temperature to 410 and 470 °C did not cause any significant changes in the IR spectra of the resulting fluoro-nanodiamond samples. The EDX analysis of these samples shows a slight increase in the fluorine content, 7.9 and 8.6 at. %, respectively, indicating that termination of the ND particle surface with fluorine has been completed at higher temperatures.

XPS studies, performed on the nanodiamond sample fluorinated at 310 °C, confirm the formation of a covalent C−F bonds and the fluorine content measured by EDX analysis. The deconvolution of the C 1s peak, shown in Figure 2, results in two features. The major feature, observed at 287.0 eV, characterizes the sp^3-bonded carbons located in the positions adjacent to fluorinated carbons. The minor component, occurring at

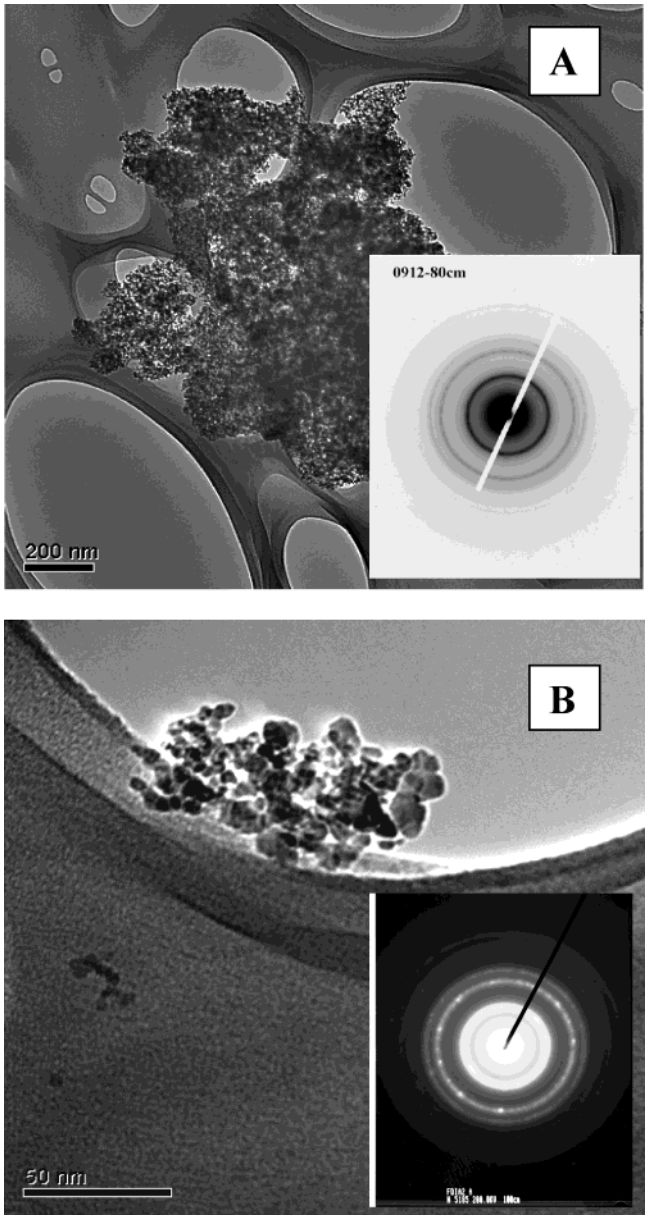

Figure 3. TEM images and corresponding SAD patterns (insets) of nanodiamond specimen taken before (A) and after fluorination at 310 °C (B).

288.9 eV, can be assigned to the carbon atoms covalently bonded to fluorine.[32] The presence of low amounts of surface oxygen was also observed in the survey spectrum. The binding energies for the carbon atoms in the fluoro-nanodiamond agree with the XPS data previously established for the carbons located in the similar bonding environments in the fluorinated polycrystalline diamond powder[30] and cagelike $C_{60}F_x$ (x = 36, 48) derivatives.[36]

The TEM images obtained for pristine ND powder and fluro-nanodiamond specimen are compared in Figure 3. They show the identical SED patterns for both solids, typical for cubic nanocrystalline diamond, which indicate that the fluorination has modified only the nanodiamond surface leaving the particle core structure intact. However, comparison of TEM images A and B

(35) Roeges, N. P. G. *Guide to the Complete Interpretation of Infrared Spectra of Organic Structures*; Wiley Publ.: Chichester, England, 1994.

(36) Kawasaki, S.; Aketa, T.; Touhara, H.; Okino, F.; Boltalina, O. V.; Gol'dt, I. V.; Troyanov, S. I.; Taylor, R. *J. Phys. Chem. B* **1999**, *103*, 1223.

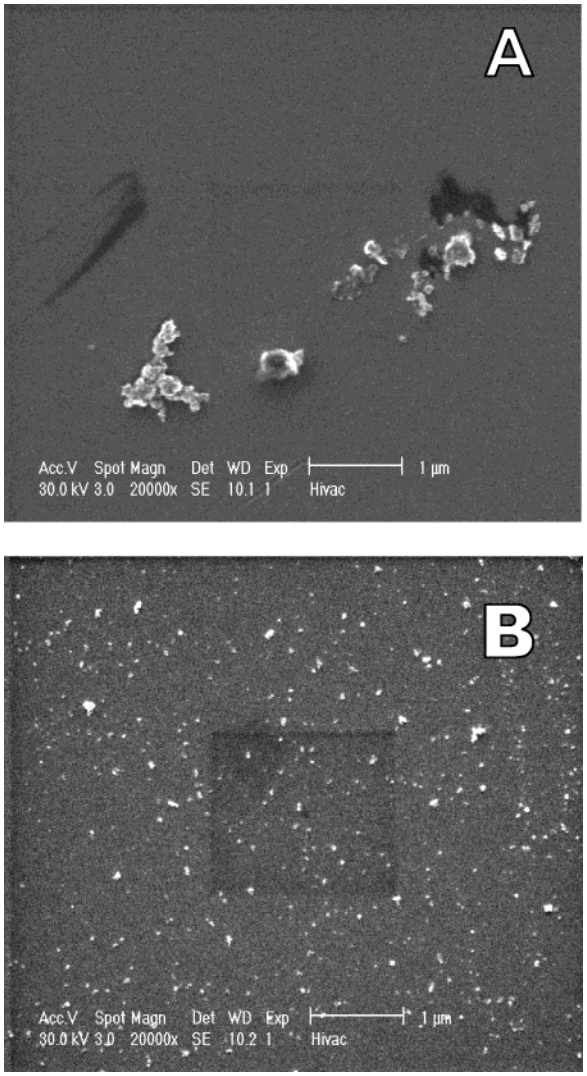

Figure 4. SEM images of nanodiamond samples taken before (A) and after fluorination (B).

shows that the surface modification dramatically affects the aggregate particle size, which after fluorination is reduced by more than 10 times from the micrometer to tens of nanometers scale. Similarly, the aggregate particle size reduction by surface fluorination was also observed by SEM imaging of the solid samples deposited on copper substrate from sonicated powder suspensions in ethanol. The pristine ND clusters (Figure 4A) appear to be drastically deagglomerated after transformation into fluoro-nanodiamond which is shown to consist of tiny nanoparticles (Figure 4B).

Derivatization of Fluoro-Nanodiamond. In this work we have found that, similar to recently studied fluoro-nanotube derivatization reactions,[37,38] the C−F bonds in fluoro-nanodiamond **1** can also react with strong nucleophilic reagents, producing new nanodiamond derivatives. Thus, interactions of **1** with the alkyllithium reagents RLi (R = CH_3, *n*-C_4H_9, *n*-C_6H_{13}) lead to methyl-, *n*-butyl-, and hexyl-nanodiamond derivatives **2a**−**c**, respectively, while reactions with ethylenediamine and glycine ethyl ester hydrochloride result in amino-nanodiamond **(2d)** and glycine-nanodiamond **(2e)** (Scheme 1). The efficiency of fluorine substitution in **1** and covalent attachment of new functional groups to nanodiamond have been evidenced by a set of several materials characterization data.

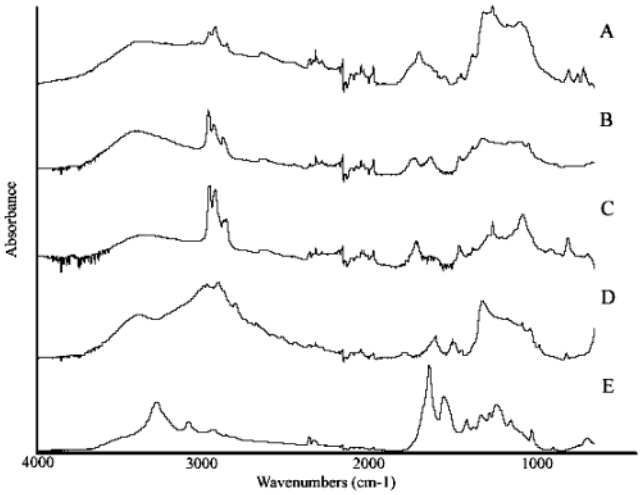

Figure 5. ATR-FTIR spectra of nanodiamond derivatives **2a** (A), **2b** (B), **2c** (C), **2d** (D), and **2e** (E).

EDX analyses of nanodiamonds derivatives **2a**−**e** yield almost zero fluorine content in alkyl-nanodiamonds **2a**−**c** and no more than 1 at. % in **2d**,**e**, which indicates the efficient displacement of fluorine in **1** and is also in line with the relative nucleophilicity of the reagents studied. The evidence for covalent attachment of new functional groups instead of fluorine is provided by the ATR-IR spectra of **2a**−**e** shown in Figure 5. In these spectra the peaks of the C−F stretching vibrations, observed in **1**, are absent. Instead, after completion of reactions with each of the nucleophilic reagents studied, new prominent peaks appear in the 2800−2980 and 800−1450 cm^{-1} spectral regions due to the C−H stretching and deformation modes as a result of fluorine displacement. In the spectrum of amino-nanodiamond **2d** (Figure 5D), an additional broad peak at 3360−3400 cm^{-1} and a medium-intensity peak at 1630 cm^{-1} can be related to the N−H stretches and NH_2 scissor motion, respectively, of *N*-ethyleneamino group attached to the nanodiamond surface. The IR spectrum of glycine-nanodiamond **2e** indicates that the ethyl ester protecting group has been removed during the derivatization reaction, since the band of ester carbonyl stretch is absent and spectral features of the covalently attached glycine amino acid appear in the range typical for the zwitterionic structure ($-NH_2^+CH_2COO^-$) of this moiety.[39] This is evidenced by the observation of asymmetric and symmetric N−H stretches at 3280 and 3088 cm^{-1}, respectively, and of the bands of carboxylate anion stretching modes at 1642 and 1554 cm^{-1}.

Thermal degradation analysis (TGA) coupled with the on-line monitoring of volatile products by a mass spectrometer (MS) gave further evidence for covalent surface functionalization of nanodiamond. The TGA-MS experiment was carried out with 30 mg of hexyl-nanodiamond **2c** placed into a TGA pen and heated at

(37) Khabashesku, V. N.; Billups, W. E.; Margrave, J. L. *Acc. Chem. Res.* **2002**, *35*, 1087.

(38) Khabashesku, V. N. Chemistry of Carbon Nanotubes. In *Encyclopedia of Nanoscience and Nanotechnology*; Nalwa, S., Ed.; American Scientific Publishers: Los Angeles, CA, 2004; Vol. 1, p 849.

(39) *The Aldrich Library of Infrared Spectra*, 2nd ed.; Pouchert, C. J., Ed.; Milwaukee, WI, 1975.

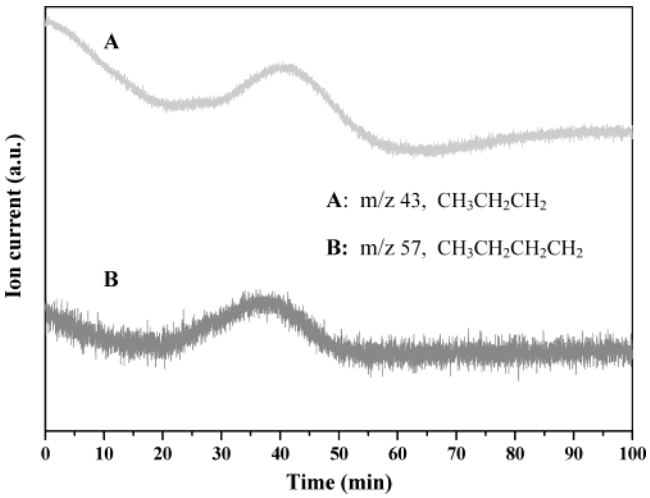

Figure 6. Ion current vs time (temperature) curves from thermal degradation TG-MS studies of hexyl-nanodiamond (**2c**).

10 °C/min to 600 °C in the flow of argon. The ion current vs time curves for the ions originating from the evoluted products detaching from the **2c** hexyl groups are presented in Figure 6. The A and B evolution curves were obtained for the detaching fragments observed at *m*/*z* = 57 ($CH_3CH_2CH_2CH_2$) and *m*/*z* = 43 ($CH_3CH_2CH_2$), respectively. Each curve exhibits a peak in the 250−400 °C range. The appearance of these peaks at such high temperatures shows that this is not caused by the evolution of physisorbed species. These peaks also appear at the same temperature which indicates that both fragments originate from the same parent molecular ion. Although the heavier fragment ions of hexane, such as those at *m*/*z* 85 and 71, were not clearly detected because of the limited sensitivity of the mass spectrometer, the identification of hexane is supported by the literature data showing that the ions with *m*/*z* 57 and 43 are the most abundant in the mass spectrum of hexane.[40]

The subsequent derivatizations of fluoro-nanodiamond studied in this work most likely involve only the surface chemical bonds and therefore do not affect the underlying crystalline structure. For instance, the cubic XRD pattern of the nanodiamond powder,[41] shown in Figure 7A, remains virtually unchanged by the derivatization reactions, which is in agreement with the observed identical microdiffraction patterns in the TEM of ND and functionalized ND **1** (Figure 3). This is also demonstrated by the XRD "fingerprints" of hexyl-nanodiamond **2c** taken as an example (Figure 7B). The average size of nanocrystals (∼3.5 nm) in ND powder, estimated from the half-widths of XRD peaks by using Scherrer equation, was not affected by the surface chemical functionalization, e.g., in **2c** derivative. TEM images (Figure 3) also show the clusterlike specimen of these powders consisting of tiny (∼3−5 nm) sphere-shaped nanocrystals.

Solubility. It is always regarded that pristine nanodiamond powder is almost insoluble in most common solvents since complete precipitation of all dispersed

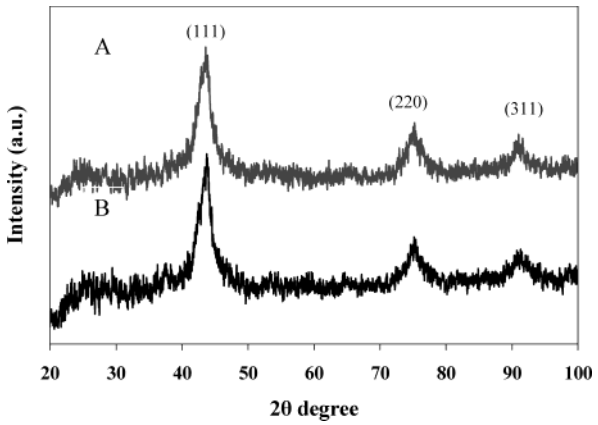

Figure 7. XRD patterns of nanodiamond powder (A) and hexyl-nanodiamond (**2c**) (B).

Table 1. Solubility (mg/L) of Pristine ND and Fluoro- and Hexyl-Nanodiamond Derivatives in Organic Solvents

solvent	pristine ND	fluoro-ND (**1**)	hexyl-ND (**2c**)
ethanol	22.5	47.5	55.6
2-propanol	27.5	42.5	49.4
thf	6.2	55.0	26.3
acetone	0	30.0	31.3
chloroform	5.0	43.8	32.5

particles from some solutions is already observed after a few hours. In this work we have demonstrated that solubility of nanodiamond can be significantly improved through functionalization. The suspension solutions formed can stand without any precipitation for several weeks or even longer at reduced concentrations. Quantitative estimation of the solvation of functionalized nanodiamonds was performed for derivatives **1** and **2c** by dispersing 20 mg of these derivatives in 200 mL of selected solvent by using sonication for 2 h. Thereafter, the dispersion formed was left to settle for 2 days. The top 150 mL of the solution, containing most "dissolved" sample, was decanted and the solvent evaporated. The obtained solid residue was weighed and the solubility calculated in mg/L. The accordingly obtained solubility data on **1** and **2c**, compared to those similarly produced for pristine ND, are presented in Table 1. They show that THF is the best solvent for fluoro-nanodiamond, while alcohols (ethanol and 2-propanol) can serve as good solvents for both functionalized nanodiamonds, **1** and **2c**, forming suspension solutions stable for many weeks without any visible precipitation. However, the same organic solvents, listed in Table 1, provide a less stable suspension media for pristine ND. After 2 h sonication full ND precipitation was observed from acetone just within a few hours and took longer (∼72 h) when other polar solvents were used (Table 1).

We have also found that fluorination and subsequent derivatization chemical processing of nanodiamond powder can assist in reducing the agglomeration of clusters in the solution phase. This effect has been observed by DLS measurements of the particle size distribution in the ethanol suspension solutions of pristine nanodiamond and its derivatives **1** and **2c**−**e** after 2 h of sonication. The measured size distribution curves are shown in Figure 8. Comparison of the curves obtained for pristine nanodiamond and fluoro-nanodiamond (Figure 8A) solutions demonstrate more than 10 times mean aggregated particle size (APS) reduction

(40) Stenhagen, E.; Abrahamsson, S.; McLafferty, F. W. *Atlas of Mass Spectral Data*; Interscience Publ.: New York, 1969; Vol. 1.
(41) Chen, J.; Deng, S. Z.; Chen, J.; Yu, Z. X.; Xu, N. S. *Appl. Phys. Lett.* **1999**, *74*, 3651.

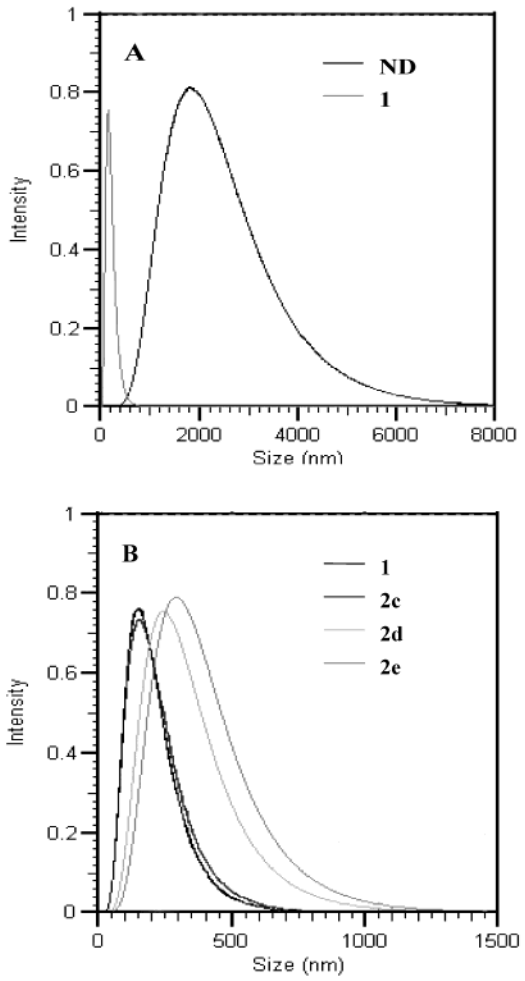

Figure 8. DLS particle size distribution curves for ethanol suspension solutions of pristine nanodiamond powder and fluoro-nanodiamond (A) and nanodiamond derivatives **1** and **2c**−**e** (B).

due to surface bonded fluorine, from 1930 nm in ND to 160 nm in **1**. The substitution of fluorine by nonpolar hexyl groups does not significantly change the APS distribution, yielding a mean size value of 168 nm for **2c**. However, introduction of polar groups capable of dipole−dipole and hydrogen-bonding interactions facilitates the enlargement of mean APS to 262 nm in the amino-nanodiamond **2d** and to 310 nm in the glycine-nanodiamond **2e**, as compared to fluoro-nanodiamond (Figure 8B). Nevertheless, for all functionalized nanodiamonds the mean APS in solutions were found to be at least 6−12 times smaller than in the pristine nanodiamond suspensions. The solvation and cluster size properties, improved by the functionalization methodology developed in this work, will certainly help to extend the applications of nanodiamond powder to many new nanoengineering and biomedical areas.

Conclusion

We have demonstrated an efficient two-step method for covalent surface functionalization of less expensive than CVD-diamond commercial nanoscale diamond powders through fluorination and subsequent derivatization with a number of functional groups. The direct fluorination procedure for nanodiamond, developed in this work, utilizes relatively low temperatures (150−310 °C) and does not require a pretreatment of the powder by hydrogen at substantially higher temperatures. The product of direct fluorination, fluoro-nanodiamond, is soluble in organic polar solvents and can be used as a precursor for further surface modification through wet chemistry fluorine substitution reactions with nucleophilic reagents; e.g., terminal amino and carboxyl groups in the derivatives **2d**,**e** can serve as binding sites for integration into epoxy polymer composites used for hardened corrosion resistant coatings. The improved solubility of the functionalized nanodiamonds will facilitate these engineering applications as well as biomedical applications through the attachment of more complex molecules (such as proteins and DNA). The solvation and reduced agglomeration of nanodiamond particles achieved through the surface functionalization in this work strongly encourage further studies of the chemistry and properties of nanodiamond powder, which are to be continued.

Acknowledgment. This work was supported by the Texas Advanced Technology Program and The Robert A. Welch Foundation of Texas. We thank Mr. B. Brinson and Dr. H. Peng for assistance in TEM imaging, Mr. Raj Wahi for assistance in collecting XRD data, and Prof. E. N. Yakovlev for helpful discussions.

CM048875Q